Faraday Discussions
Cite this: *Faraday Discuss.*, 2025, **255**, 483

PAPER

Exploring the crystallisation of aspirin in a confined porous material using solid-state nuclear magnetic resonance†

Marie Juramy, ‡[a] Eric Besson,[a] Stéphane Gastaldi, [a] Fabio Ziarelli, [b] Stéphane Viel, [ac] Giulia Mollica [a] and Pierre Thureau *[a]

Received 3rd June 2024, Accepted 16th July 2024
DOI: 10.1039/d4fd00123k

In this study, nuclear magnetic resonance (NMR) is used to investigate the crystallisation behaviour of aspirin within a mesoporous SBA-15 silica material. The potential of dynamic nuclear polarisation (DNP) experiments is also investigated using specifically designed porous materials that incorporate polarising agents within their walls. The formation of the metastable crystalline form II is observed when crystallisation occurs within the pores of the mesoporous structure. Conversely, bulk crystallisation yields the most stable form, namely form I, of aspirin. Remarkably, the metastable form II remains trapped within the pores of mesoporous SBA-15 silica material even 30 days after impregnation, underscoring its persistent stability within this confined environment.

Introduction

Despite the significance of crystallisation phenomena in various fields such as chemistry, materials science, and biology (*e.g.* biomineralization), gaining a comprehensive understanding of these processes can often be challenging.[1–4] In fact, the intricate mechanistic pathway that leads from molecules dispersed in a solution to the formation of the initial crystalline assembly (referred to as the critical nucleation cluster) and subsequent growth towards the final crystalline phase is a complex phenomenon. Additionally, the process can be further complicated by the evolution of the system through different temporary phases, such as amorphous phases or metastable polymorphs, before achieving the desired crystallisation product. A thorough comprehension of the complete

[a]*Aix-Marseille Univ., CNRS, ICR UMR 7273, 13397 Marseille, France. E-mail: pierre.thureau@univ-amu.fr*
[b]*Aix-Marseille Univ., Centrale Mediterranée, CNRS, Fédération des Sciences Chimiques FR 1739, 13397 Marseille, France*
[c]*Institut Universitaire de France, 75005 Paris, France*

† Electronic supplementary information (ESI) available. See DOI: https://doi.org/10.1039/d4fd00123k

‡ Present address: Yusuf Hamied Department of Chemistry, University of Cambridge, Cambridge CB2 1EW, U.K.

mechanistic pathway is crucial for advancing our knowledge of crystallisation processes and serves as a prerequisite for devising experimental strategies to effectively control the formation of specific polymorphs. Unfortunately, the observation of metastable crystalline forms can sometimes be difficult.

For example, aspirin, alternatively also known as acetyl salicylic acid, is a long-standing medicinal drug that exists in various forms. The initial crystal structure of aspirin was determined in 1964 while the polymorphism of aspirin has long been speculated based on notable disparities in melting point and dissolution rates during experimental measurements.[5,6]

Subsequently, in 2004, Ouvrard and Price made a prediction regarding the presence of a second crystal structure of aspirin using crystal structure prediction techniques.[7] Following this, experimental observation[8] and successful crystal structure determination were achieved for form II of aspirin.[9] Subsequently, Bond *et al.* confirmed the crystal structure by performing X-ray diffraction on higher purity crystals and showed that form I (*i.e.*, the most stable form of aspirin) and form II had very similar structures.[10] Hence, it is likely that forms I and II existed as inter-grown crystals.[11] Later, in 2017, a third form of aspirin, known as form IV, was obtained from molten aspirin.[12]

In 2019, Peksa *et al.* explored the crystallisation of aspirin within the pores of porous glass composites characterized by different pore sizes. Raman spectroscopy and differential scanning calorimetry (DSC) experiments allowed them to identify that distinct crystalline forms of aspirin were present within the pores of the material.[13] In fact, it is widely established that the process of crystallisation occurring within nanopores has the ability to generate and stabilize polymorphs that would otherwise be metastable under typical bulk crystallisation conditions.[3,14–16]

In this study, we used nuclear magnetic resonance (NMR) to study the crystallisation of aspirin within the pores of a mesoporous SBA-15 silica material. In fact, the precise measurement of solid-state NMR chemical shifts[17–26] allowed for reliable identification of the different solid forms (*e.g.* polymorphs) present during crystallisation processes.[27–29] However, it is worth noting that transient solid forms, which are typically present in minimal quantities, may not be detectable in NMR studies due to the inherently low sensitivity of the technique, thereby resulting in the potential inability to observe short-lived intermediate phases.

To address these challenges, employing low-temperature solid-state NMR and dynamic nuclear polarisation (DNP) experiments can prove to be a valuable strategy.[30,31] In principle, using low temperatures can trap transient forms, while DNP experiments can overcome the inherent challenges associated with the low sensitivity of NMR, especially when monitoring transient forms.[32,33]

In DNP experiments, microwave radiation is applied to the sample, facilitating the transfer of electron spin polarisation from unpaired electrons to the nuclear spins, thereby enhancing the strength of the NMR signal.[34–42] However, the addition of paramagnetic polarising agents[43–51] to the typically diamagnetic sample may alter the properties of the system being investigated, posing a potential concern when applying DNP experiments to the study of crystallisation processes. Usually, the polarising agents are dissolved in specific solvents, such as water/glycerol or tetrachloroethane, to promote glass formation during freezing, which helps to maximise the efficiency of DNP by ensuring a homogeneous

dispersion of the radical across the sample. Nevertheless, using glass forming agents in crystallisation experiments can potentially impact the outcome of the crystallisation process.[52,53]

In the case of crystallisation processes occurring in confined conditions, these issues can be overcome by integrating the polarising agent within the walls of nanostructured porous materials.[54–56] This ensures that (i) the polarising agent and the molecule undergoing crystallisation in the solution exist in separate phases, and (ii) the polarising agents are uniformly distributed throughout the entire sample. Notably, DNP polarising agents, such as TEMPO nitroxide radicals, were incorporated into the pore walls of silica materials.[54,55,57,58] Interestingly, these materials proved useful for monitoring crystallisation processes using DNP experiments.[59]

In this study, we investigated the crystallisation of aspirin within the pores of a mesoporous SBA-15 silica material, which possesses pores with a diameter of approximately 7–8 nm. Our experiments used two kinds of mesoporous SBA-15 silica materials, *i.e.* with and without polarising agents incorporated into their walls, enabling us to explore the potential of DNP experiments in the case of aspirin. Our results indicate that, under confinement, crystallisation of form II is favoured compared to bulk conditions.

Results and discussion

Fig. 1 illustrates our strategy for monitoring the crystallisation of aspirin within mesoporous SBA-15 silica material. The mesoporous material is impregnated

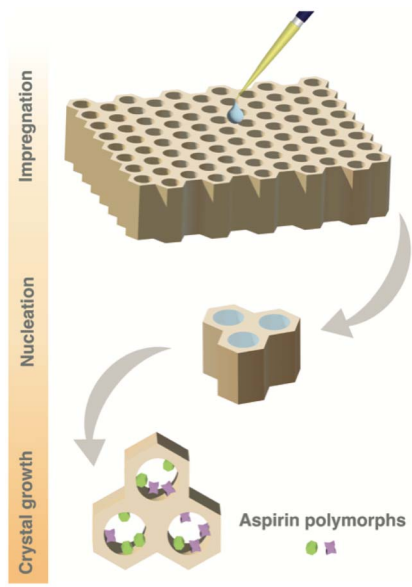

Fig. 1 Schematic representation of the crystallisation of aspirin within the pores of mesoporous SBA-15 silica material (with or without wall-embedded TEMPO radicals). The mesoporous silica material is impregnated with a solution of aspirin in ethanol (0.8 M). Evaporation of solvent (ethanol) leads to crystallisation of aspirin within the pores of the material.

with an undersaturated solution of aspirin dissolved in ethanol (0.8 M) at ambient temperature and stored in an open vial within a desiccator at a fixed humidity of 43%, allowing crystallisation to proceed through solvent evaporation. After 2 days, the material is extracted from the vial and transferred to a solid-state NMR rotor. The rotor is then inserted into the DNP solid-state NMR spectrometer at a temperature of 98 K, rapidly quenching the crystallisation process. Subsequently, no further evolution of the crystallisation process occurs, and the resulting sample represents the crystallisation system frozen at the moment of quenching. A variety of NMR experiments can then be conducted on this so-called "frozen" crystallisation system.

Concurrently, an identical solution of 0.8 M aspirin dissolved in ethanol was allowed to crystallise under bulk conditions to compare the favoured crystalline forms within confined conditions with those obtained through bulk crystallisation. After 2 days of crystallisation, ^{13}C CPMAS NMR experiments were performed on both the mesoporous silica impregnated with the aspirin/ethanol solution and the crystals obtained from bulk crystallisation. Furthermore, a ^{13}C CPMAS NMR experiment was performed on the commercial aspirin used to prepare the solution.

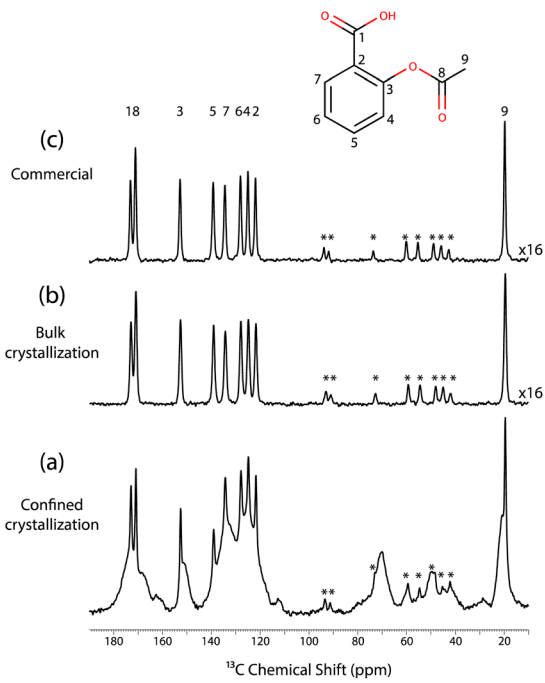

Fig. 2 (a) ^{13}C CPMAS NMR spectrum recorded for a mesoporous SBA-15 silica material without wall-embedded TEMPO radicals and impregnated at room temperature with a solution of aspirin in ethanol (0.8 M). The spectrum was recorded 2 days after impregnation. (b) ^{13}C CPMAS NMR spectrum recorded for a powder sample of aspirin subsequently obtained from a solution of aspirin in ethanol. (c) ^{13}C CPMAS NMR spectrum of commercial aspirin. All spectra were recorded without microwave irradiation and at a temperature of 98 K. Signals labelled with "*" correspond to spinning side bands.

Fig. 2 displays the ^{13}C CPMAS NMR spectra recorded at a temperature of 98 K for these three samples. Specifically, Fig. 2c corresponds to the spectrum recorded for the commercial aspirin. The observed ^{13}C chemical shifts matched with the expected ^{13}C chemical shifts of form I. Fig. 2b shows the ^{13}C CPMAS NMR spectrum recorded on the crystals obtained from the bulk crystallisation; the spectrum is identical to the ^{13}C CPMAS NMR spectrum obtained for the commercial form. Therefore, the bulk crystallisation of aspirin in ethanol also led to the formation of form I.

Finally, Fig. 2a shows the spectrum recorded on the impregnated mesoporous SBA-15 silica material, where 3 distinct phases can be observed. The sharp signals matched with the signals of both the commercial and the bulk crystals, and hence correspond to the ^{13}C NMR signals of form I. Moreover, the broad signals are probably due to the amorphous aspirin/ethanol frozen glass phase. Interestingly, a third signal is observed in the region corresponding to the methyl group, as shown in Fig. 3.

Notably, this third methyl ^{13}C NMR signal appears as a low intensity shoulder on the main peak and has a chemical shift of 20.9 ppm, which may correspond to form II of aspirin.[60,61]

In fact, it has been shown that the ^{13}C CPMAS spectra of form I and form II exhibited variations primarily in the methyl ^{13}C peak.[8,60,61] Specifically, at room temperature, the ^{13}C chemical shift of the methyl group in form I was found to be 20.0 ppm, compared to 20.7 ppm in form II. At a temperature of 105 K, the chemical shift slightly shifted with the methyl group of form I being at 19.8 ppm and form II at 20.9 ppm.[61] Importantly, it is not possible to reproduce the ^{13}C NMR spectrum shown in Fig. 3 when only two signals are used in the deconvolution, as shown in the ESI.†

As a result, the confined crystallisation of aspirin in a mesoporous SBA-15 silica material seems to have led to the detection of 3 different phases, aspirin molecules in solution, form I and form II.

It is well known that NMR allows amorphous phases to be distinguished from crystalline phases on the basis of signal line widths, with amorphous phases

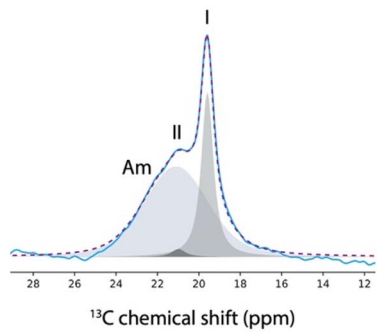

Fig. 3 ^{13}C NMR resonances corresponding to the methyl group of the aspirin spectrum (blue curve) recorded at 98 K on a mesoporous SBA-15 silica material 2 days after impregnation with a solution of aspirin in ethanol (0.8 M). The Gaussian peaks used for the deconvolution are shown as filled grey shapes and their sum is shown as a dotted purple line. The 3 Gaussian peaks correspond to the individual ^{13}C NMR resonances of the amorphous phase (Am), and the crystalline phases of form I and II of aspirin.

giving rise to significantly broader lines. In fact, the signal from amorphous phases of aspirin/ethanol frozen solution can be suppressed through a $T_{1\rho}$ relaxation filter experiment. This method relies on differences in the relaxation times of aspirin in crystalline and amorphous phases.[59,62] The $T_{1\rho}$-filtered ^{13}C CPMAS NMR spectrum is shown in Fig. 4 where the ^{13}C NMR resonances arising from the amorphous phase have been completely suppressed, whereas the ^{13}C NMR resonances corresponding to the crystalline forms I and II of aspirin are still observed. Overall, the results presented in Fig. 2–4 clearly demonstrate that form II of aspirin is formed when crystallisation occurs in a confined environment.

It should be noted that all the spectra shown in Fig. 2–4 were recorded using a mesoporous SBA-15 silica material without polarising agents incorporated into its walls. As a result, no DNP experiments were conducted in this case.

In order to assess whether DNP experiments could improve the sensitivity of NMR experiments conducted on aspirin, similar experiments were performed utilising a mesoporous SBA-15 silica material with polarising agents incorporated into its walls. In principle, under microwave irradiation, the large polarisation of the electronic spins of the TEMPO radicals located within the walls of the material should be transferred to the different phases of aspirin. Unfortunately, no DNP enhancement was observed in our case.

These results are consistent with those reported by Hanrahan *et al.*, where a relatively modest DNP enhancement of 7.5 was measured for an aspirin powder impregnated with a 16 mM solution of TEKPol in 1,3-dibromobutane.[61] The TEKPol radical typically provides much higher DNP signal enhancements than TEMPO, which may explain why we did not observe any DNP signal enhancement in our experiments. Another potential explanation for the lack of DNP enhancement in our experiment could arise from the polarisation transfer that occurs in the mesoporous SBA-15 silica material, which is still poorly understood. It may be speculated that the low density of ^{1}H spins in our inorganic materials may not correspond to the optimal polarisation transfer through ^{1}H spin diffusion from

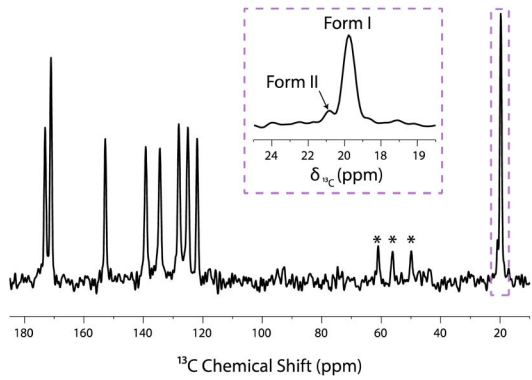

Fig. 4 $T_{1\rho}$-filtered ^{13}C CPMAS NMR spectrum recorded on a mesoporous SBA-15 silica material impregnated with a 0.8 M solution of aspirin in ethanol. This experiment was recorded 2 days after material impregnation, without microwave irradiation and at a temperature of 98 K. Signals labelled with "*" correspond to spinning side bands. The ^{13}C NMR chemical shift of the methyl group signal of forms I and II are at 19.8 ppm and 20.9 ppm, respectively.

the electronic spins located within the walls of the material towards the pores.[63] Moreover, this polarisation transfer is further reduced in our experiments by the fast rotation of the methyl groups in aspirin molecules, acting as a potential relaxation sink, thus leading to poor DNP polarisation transfer.[64–66] In fact, at a temperature of 98 K, a ^{1}H T_1 relaxation time of $\approx$3 s was measured in the case of aspirin form I. As a result, the enhanced polarisation quickly dissipates through ^{1}H relaxation before it can spread throughout the sample.[66–68]

Conclusions

Although DNP experiments performed with tailored porous materials proved ineffective in the case of aspirin, these results nonetheless demonstrate that form II of aspirin can be obtained when the crystallisation occurs within the pores of a mesoporous SBA-15 silica material. This result confirmed that unstable crystalline forms can be stabilised in a confined environment. Importantly, evaporation of ethanol from the crystallisation system does not reach completion in our experiments. For a sample left in a sealed desiccator at room temperature and fixed humidity (43%) for 30 days after impregnation, the ^{13}C CPMAS NMR spectrum recorded at 98 K still contains a broad signal due to the amorphous aspirin/ethanol frozen solution, together with sharp signals corresponding to forms I and II of aspirin. Interestingly, even 30 days after the start of crystallisation, the metastable form II of aspirin remains trapped and stabilized within the mesoporous silica material at room temperature. We also note that, although CPMAS experiments are intrinsically nonquantitative, the significant difference between the signal intensities of both forms allowed us to conclude that form II was present in a smaller amount than form I, but no attempt was made at this point to precisely quantify their respective amounts (using, for instance, multi-CP experiments).[69]

Importantly, the experimental strategy used here is confirmed to be a powerful method to reveal the existence and possibly to investigate the structure of transient crystalline forms. These forms typically evolve too rapidly in bulk solution to be detected using typical NMR measurement conditions. Moreover, this approach is adaptable for exploring various crystallising substances and solvents, offering a versatile means to gain fresh insights into a wide array of crystallisation systems. In future studies, it would be interesting to monitor whether the DNP NMR sensitivity could be improved by using alternative materials, such as porous polymers with nitroxide radicals grafted in the bulk matrix.[70] In fact, it can be anticipated that the higher ^{1}H density in this kind of porous material may yield more efficient polarisation transfer from the polarising agents towards the target, potentially enhancing the sensitivity of DNP solid-state NMR experiments for studying crystallisation in confined media.

Experimental

Mesoporous silica

The SBA-15 mesoporous silica materials were synthesized by the method of Besson *et al.* (particle size < 10 μm).[54] The mesopores have cylindrical shape (diameter 7–8 nm) and are connected through micropores.

The materials with wall-embedded TEMPO radicals were obtained through heating of the corresponding bis-alkoxyamine.[54,56] The radical concentration (0.52 ± 0.03 mmol g^{-1}) and the uniform distribution of radicals were established by electron paramagnetic resonance.[71]

DNP enhancements (εDNP) measured on a 0.2 M aqueous solution of U–$^{13}C/^{15}N$ proline were used to evaluate the radical concentration and homogeneous distribution in the SBA material. Values of εDNP measured for the material used in this study are comparable to those reported previously for SBA materials with similar radical concentrations.[54]

Sample preparation

Aspirin was purchased from Sigma-Aldrich and used without further purification. Absolute ethanol was purchased from Carlo Erba.

An undersaturated solution of aspirin (0.8 M) in ethanol was prepared in a glass vial (2 ml), at room temperature. The solution was then stirred for 10 min, until aspirin molecules were completely dissolved. The solution was passed through a 0.45 μl poly (tetrafluoroethylene) syringe filter in order to remove any insoluble particles left in the solution.

A volume of 40 μl of the aspirin solution was used to impregnate 20 mg of mesoporous silica material. The amount of aspirin solution used for impregnation was approximately equal to the total pore volume of the mesoporous material, based on the total mass and specific surface area of the material (determined by the Brunauer–Emmett–Teller (BET) method), while the pore size distribution was calculated from desorption isotherms using the Barrett–Joyner–Halenda (BJH) method. This procedure maximises the loading of aspirin within the pores while minimizing the residual amount of aspirin on the exterior surfaces of the mesoporous material.

The sample was stored in a glass vial (2 ml) left open in a desiccator at a humidity level of 43% and a temperature of 22 °C. Humidity was controlled by a supersaturated aqueous solution of potassium carbonate. A few days after impregnation of the silica (*i.e.*, 2 days), the sample was packed in a 3.2 mm sapphire rotor and quenched in the MAS DNP spectrometer at 100 K in order to identify the crystalline form of aspirin favoured under confined conditions. The remaining 110 μl of the solution of aspirin was stored in a glass vial (2 ml) left open in a desiccator at a humidity level of 43% and a temperature of 22 °C. A few days later, when the crystals are formed (*i.e.*, 2 days), the crystals were packed in a 3.2 mm sapphire rotor and quenched in the MAS DNP spectrometer at 100 K in order to identify the crystalline form of aspirin favoured under bulk conditions in ethanol.

NMR experiments

DNP solid-state NMR experiments were carried out on a Bruker 9.4 T wide-bore magnet (^1H and ^{13}C Larmor frequencies were 400 MHz and 100 MHz, respectively) operated using an AVANCE-III HD spectrometer and equipped with a Bruker 3.2 mm low-temperature double-resonance DNP $^1H/\{^{29}Si–^{13}C\}$ CPMAS probe with MAS frequency of 8 kHz. The spectrometer was equipped with a microwave source, a gyrotron, allowing the microwave irradiation of the sample. The field sweep coil of the NMR magnet was set so that the microwave irradiation

corresponds to the maximum DNP enhancement of AMUPol (*i.e.*, 263.334 GHz). At the output of the probe waveguide, the estimated power of the microwave beam was 4 W.

The ^{1}H–^{13}C CPMAS experiments NMR spectra were recorded with a MAS frequency of 8 kHz (*i.e.*, standard MAS frequency for MAS DNP experiments performed with 3.2 mm probe). The ^{1}H 90 °C pulse duration was 2.5 μs. ^{1}H decoupling was performed using SPINAL64 and with a nutation frequency of 100 kHz. The contact time was set to 2 ms and the contact pulse on ^{1}H was linearly ramped from 60 to 90 kHz. The ^{1}H T_1 relaxation time was measured using a saturation–recovery ^{1}H–^{13}C CP pulse sequence. The ^{1}H–^{13}C CPMAS spectra were recorded with a relaxation delay of 9 s and 7168 repetitions.

The $T_{1\rho}$-filtered ^{1}H–^{13}C CPMAS experiment was performed using the same parameters as the ^{1}H–^{13}C CPMAS experiment and with a ^{1}H spinlock r. f. field amplitude of 40 kHz and a duration $\tau_{SL} = 20$ ms.

Data availability

ESI† contains the signal deconvolution of the data shown in Fig. 3 using only 2 Gaussian peaks. The raw data presented in the manuscript is available at **https://doi.org/10.5281/zenodo.12688845**.

Conflicts of interest

There are no conflicts to declare.

Acknowledgements

This project received funding from ERC under the European Union Horizon 2020 research and innovation programme (Grant Agreement No. 758498). The authors acknowledge the Agence Nationale de la Recherche for funding (ANR-18-CE29-007).

References

1 J. Bernstein, *Polymorphism in Molecular Crystals*, Oxford University Press, Oxford, 2002.
2 B. Rodríguez-Spong, C. P. Price, A. Jayasankar, A. J. Matzger and N. R. Rodríguez-Hornedo, *Adv. Drug Delivery Rev.*, 2004, **56**, 241–274.
3 A. Y. Lee, D. Erdemir and A. S. Myerson, *Annu. Rev. Chem. Biomol. Eng.*, 2011, **2**, 259–280.
4 S. M. Woodley, G. M. Day and R. Catlow, *Philos. Trans. R. Soc., A*, 2020, **378**, 20190600.
5 A. G. Mitchell and D. J. Saville, *J. Pharm. Pharmacol.*, 1967, **19**, 729–734.
6 R. Tawashi, *Science*, 1968, **160**, 76.
7 C. Ouvrard and S. L. Price, *Cryst. Growth Des.*, 2004, **4**, 1119–1127.
8 E. J. Munson, *presented in part at Polymorphism in Crystals, ACS ProSpectives Conference Series*, Tampa, FL, 2004.
9 P. Vishweshwar, J. A. McMahon, M. Oliveira, M. L. Peterson and M. J. Zaworotko, *J. Am. Chem. Soc.*, 2005, **127**, 16802–16803.

10 A. D. Bond, R. Boese and G. R. Desiraju, *Angew. Chem., Int. Ed.*, 2007, **46**, 615–617.
11 E. J. Chan, T. R. Welberry, A. P. Heerdegen and D. J. Goossens, *Acta Crystallogr., Sect. B: Struct. Sci.*, 2010, **66**, 696–707.
12 A. G. Shtukenberg, C. T. Hu, Q. Zhu, M. U. Schmidt, W. Xu, M. Tan and B. Kahr, *Cryst. Growth Des.*, 2017, **17**, 3562–3566.
13 P. Peksa, J. Trzmiel, M. Ptak, M. Kostrzewa, R. Szatanik, A. Barascu, D. Enke and A. Sieradzki, *J. Mater. Sci.*, 2019, **54**, 404–413.
14 B. D. Hamilton, J.-M. Ha, M. A. Hillmyer and M. D. Ward, *Acc. Chem. Res.*, 2012, **45**, 414–423.
15 F. C. Meldrum and C. O'Shaughnessy, *Adv. Mater.*, 2020, **32**, 2001068.
16 N. Fellah, I. J. C. Dela Cruz, B. G. Alamani, A. G. Shtukenberg, A. V. Pandit, M. D. Ward and A. S. Myerson, *Cryst. Growth Des.*, 2024, **24**, 3527–3558.
17 L. E. Díaz, L. Frydman, A. C. Olivieri and B. Frydman, *Anal. Lett.*, 1987, **20**, 1657–1666.
18 R. K. Harris, *Analyst*, 2006, **131**, 351–373.
19 J. M. Griffin, D. R. Martin and S. P. Brown, *Angew. Chem., Int. Ed.*, 2007, **46**, 8036–8038.
20 M. Geppi, G. Mollica, S. Borsacchi and C. A. Veracini, *Appl. Spectrosc. Rev.*, 2008, **43**, 202–302.
21 P. Cerreia Vioglio, G. Mollica, M. Juramy, C. E. Hughes, P. A. Williams, F. Ziarelli, S. Viel, P. Thureau and K. D. M. Harris, *Angew. Chem., Int. Ed.*, 2018, **57**, 6619–6623.
22 P. Hodgkinson, *Prog. Nucl. Magn. Reson. Spectrosc.*, 2020, **118–119**, 10–53.
23 R. Mathew, K. A. Uchman, L. Gkoura, C. J. Pickard and M. Baias, *Magn. Reson. Chem.*, 2020, **58**, 1018–1025.
24 T. Whewell, V. R. Seymour, K. Griffiths, N. R. Halcovitch, A. V. Desai, R. E. Morris, A. R. Armstrong and J. M. Griffin, *Magn. Reson. Chem.*, 2022, **60**, 489–503.
25 M. Cordova and L. Emsley, *J. Am. Chem. Soc.*, 2023, **145**, 16109–16117.
26 M. Rahman, H. R. W. Dannatt, C. D. Blundell, L. P. Hughes, H. Blade, J. Carson, B. P. Tatman, S. T. Johnston and S. P. Brown, *J. Phys. Chem. A*, 2024, **128**, 1793–1816.
27 C. E. Hughes, P. A. Williams, T. R. Peskett and K. D. M. Harris, *J. Phys. Chem. Lett.*, 2012, **3**, 3176–3181.
28 C. E. Hughes, P. A. Williams, V. L. Keast, V. G. Charalampopoulos, G. R. Edwards-Gau and K. D. M. Harris, *Faraday Discuss.*, 2015, **179**, 115–140.
29 K. D. M. Harris, C. E. Hughes, P. A. Williams and G. R. Edwards-Gau, *Acta Crystallogr., Sect. C: Cryst. Struct. Commun.*, 2017, **73**, 137–148.
30 J. Jeon, W.-M. Yau and R. Tycko, *J. Am. Chem. Soc.*, 2020, **142**, 21220–21232.
31 T. Schmidt, J. Jeon, W.-M. Yau, C. D. Schwieters, R. Tycko and G. M. Clore, *Proc. Natl. Acad. Sci. U. S. A.*, 2022, **119**, e2122308119.
32 P. Vioglio Cerreia, P. Thureau, M. Juramy, F. Ziarelli, S. Viel, P. A. Williams, C. E. Hughes, K. D. M. Harris and G. Mollica, *J. Phys. Chem. Lett.*, 2019, **10**, 1505–1510.
33 M. Juramy, P. C. Vioglio, F. Ziarelli, S. Viel, P. Thureau and G. Mollica, *Solid State Nucl. Magn. Reson.*, 2022, **122**, 101836.
34 Q. Z. Ni, E. Daviso, T. V. Can, E. Markhasin, S. K. Jawla, T. M. Swager, R. J. Temkin, J. Herzfeld and R. G. Griffin, *Acc. Chem. Res.*, 2013, **46**, 1933–1941.

35 A. J. Rossini, A. Zagdoun, M. Lelli, A. Lesage, C. Copéret and L. Emsley, *Acc. Chem. Res.*, 2013, **46**, 1942–1951.
36 A. J. Rossini, *J. Phys. Chem. Lett.*, 2018, **9**, 5150–5159.
37 L. Zhao, A. C. Pinon, L. Emsley and A. J. Rossini, *Magn. Reson. Chem.*, 2018, **56**, 583–609.
38 A. G. M. Rankin, J. Trébosc, F. Pourpoint, J.-P. Amoureux and O. Lafon, *Solid State Nucl. Magn. Reson.*, 2019, **101**, 116–143.
39 R. W. Hooper, B. A. Klein and V. K. Michaelis, *Chem. Mater.*, 2020, **32**, 4425–4430.
40 T. Biedenbänder, V. Aladin, S. Saeidpour and B. Corzilius, *Chem. Rev.*, 2022, **122**, 9738–9794.
41 W. Y. Chow, G. De Paëpe and S. Hediger, *Chem. Rev.*, 2022, **122**, 9795–9847.
42 I. B. Moroz and M. Leskes, *Annu. Rev. Mater. Res.*, 2022, **52**, 25–55.
43 C. Song, K.-N. Hu, C.-G. Joo, T. M. Swager and R. G. Griffin, *J. Am. Chem. Soc.*, 2006, **128**, 11385–11390.
44 C. Sauvée, M. Rosay, G. Casano, F. Aussenac, R. T. Weber, O. Ouari and P. Tordo, *Angew. Chem., Int. Ed.*, 2013, **52**, 10858–10861.
45 A. Zagdoun, G. Casano, O. Ouari, M. Schwarzwälder, A. J. Rossini, F. Aussenac, M. Yulikov, G. Jeschke, C. Copéret, A. Lesage, P. Tordo and L. Emsley, *J. Am. Chem. Soc.*, 2013, **135**, 12790–12797.
46 G. Mathies, M. A. Caporini, V. K. Michaelis, Y. Liu, K.-N. Hu, D. Mance, J. L. Zweier, M. Rosay, M. Baldus and R. G. Griffin, *Angew. Chem., Int. Ed.*, 2015, **54**, 11770–11774.
47 D. Wisser, G. Karthikeyan, A. Lund, G. Casano, H. Karoui, M. Yulikov, G. Menzildjian, A. C. Pinon, A. Purea, F. Engelke, S. R. Chaudhari, D. Kubicki, A. J. Rossini, I. B. Moroz, D. Gajan, C. Copéret, G. Jeschke, M. Lelli, L. Emsley, A. Lesage and O. Ouari, *J. Am. Chem. Soc.*, 2018, **140**, 13340–13349.
48 A. Lund, G. Casano, G. Menzildjian, M. Kaushik, G. Stevanato, M. Yulikov, R. Jabbour, D. Wisser, M. Renom-Carrasco, C. Thieuleux, F. Bernada, H. Karoui, D. Siri, M. Rosay, I. V. Sergeyev, D. Gajan, M. Lelli, L. Emsley, O. Ouari and A. Lesage, *Chem. Sci.*, 2020, **11**, 2810–2818.
49 R. Yao, D. Beriashvili, W. Zhang, S. Li, A. Safeer, A. Gurinov, A. Rockenbauer, Y. Yang, Y. Song, M. Baldus and Y. Liu, *Chem. Sci.*, 2022, **13**, 14157–14164.
50 R. Harrabi, T. Halbritter, F. Aussenac, O. Dakhlaoui, J. van Tol, K. K. Damodaran, D. Lee, S. Paul, S. Hediger, F. Mentink-Vigier, S. T. Sigurdsson and G. De Paëpe, *Angew. Chem., Int. Ed.*, 2022, **61**, e202114103.
51 T. Halbritter, R. Harrabi, S. Paul, J. van Tol, D. Lee, S. Hediger, S. T. Sigurdsson, F. Mentink-Vigier and G. De Paëpe, *Chem. Sci.*, 2023, **14**, 3852–3864.
52 R. J. Davey, S. L. M. Schroeder and J. H. ter Horst, *Angew. Chem., Int. Ed.*, 2013, **52**, 2166–2179.
53 E. Meirzadeh, S. Dishon, I. Weissbuch, D. Ehre, M. Lahav and I. Lubomirsky, *Angew. Chem., Int. Ed.*, 2018, **57**, 4965–4969.
54 E. Besson, F. Ziarelli, E. Bloch, G. Gerbaud, S. Queyroy, S. Viel and S. Gastaldi, *Chem. Commun.*, 2016, **52**, 5531–5533.
55 D. L. Silverio, H. A. van Kalkeren, T.-C. Ong, M. Baudin, M. Yulikov, L. Veyre, P. Berruyer, S. Chaudhari, D. Gajan, D. Baudouin, M. Cavaillès, B. Vuichoud,

A. Bornet, G. Jeschke, G. Bodenhausen, A. Lesage, L. Emsley, S. Jannin, C. Thieuleux and C. Copéret, *Helv. Chim. Acta*, 2017, **100**, e1700101.
56 P. Nabokoff, G. Brulay, C. Dol, G. Gerbaud, B. Guigliarelli, E. Etienne, E. Bloch, F. Ziarelli, E. Besson and S. Gastaldi, *J. Phys. Chem. C*, 2023, **127**, 9699–9706.
57 M. Cavaillès, A. Bornet, X. Jaurand, B. Vuichoud, D. Baudouin, M. Baudin, L. Veyre, G. Bodenhausen, J.-N. Dumez, S. Jannin, C. Copéret and C. Thieuleux, *Angew. Chem., Int. Ed.*, 2018, **57**, 7453–7457.
58 E. Besson, A. Vebr, F. Ziarelli, E. Bloch, G. Gerbaud, S. Queyroy, P. Thureau, S. Viel and S. Gastaldi, *Phys. Chem. Chem. Phys.*, 2022, **24**, 25279–25286.
59 M. Juramy, R. Chèvre, P. Cerreia Vioglio, F. Ziarelli, E. Besson, S. Gastaldi, S. Viel, P. Thureau, K. D. M. Harris and G. Mollica, *J. Am. Chem. Soc.*, 2021, **143**, 6095–6103.
60 D. Sperger, *PhD Dissertation*, University of Kansas, 2010.
61 M. P. Hanrahan, A. Venkatesh, S. L. Carnahan, J. L. Calahan, J. W. Lubach, E. J. Munson and A. J. Rossini, *Phys. Chem. Chem. Phys.*, 2017, **19**, 28153–28162.
62 J. R. Yarava, S. R. Chaudhari, A. J. Rossini, A. Lesage and L. Emsley, *J. Magn. Reson.*, 2017, **277**, 149–153.
63 O. Lafon, A. S. L. Thankamony, T. Kobayashi, D. Carnevale, V. Vitzthum, I. I. Slowing, K. Kandel, H. Vezin, J.-P. Amoureux, G. Bodenhausen and M. Pruski, *J. Phys. Chem. C*, 2013, **117**, 1375–1382.
64 G. Mollica, D. Le, F. Ziarelli, G. Casano, O. Ouari, T. N. T. Phan, F. Aussenac, P. Thureau, D. Gigmes, P. Tordo and S. Viel, *ACS Macro Lett.*, 2014, **3**, 922–925.
65 A. C. Pinon, A. J. Rossini, C. M. Widdifield, D. Gajan and L. Emsley, *Mol. Pharm.*, 2015, **12**, 4146–4153.
66 A. Zagdoun, A. J. Rossini, M. P. Conley, W. R. Grüning, M. Schwarzwälder, M. Lelli, W. T. Franks, H. Oschkinat, C. Copéret, L. Emsley and A. Lesage, *Angew. Chem., Int. Ed.*, 2013, **52**, 1222–1225.
67 A. Abragam, *Principles of Nuclear Magnetism*, Oxford University Press, Oxford, 1961.
68 A. J. Rossini, A. Zagdoun, F. Hegner, M. Schwarzwälder, D. Gajan, C. Copéret, A. Lesage and L. Emsley, *J. Am. Chem. Soc.*, 2012, **134**, 16899–16908.
69 R. L. Johnson and K. Schmidt-Rohr, *J. Magn. Reson.*, 2014, **239**, 44–49.
70 T. El Daraï, S. F. Cousin, Q. Stern, M. Ceillier, J. Kempf, D. Eshchenko, R. Melzi, M. Schnell, L. Gremillard, A. Bornet, J. Milani, B. Vuichoud, O. Cala, D. Montarnal and S. Jannin, *Nat. Commun.*, 2021, **12**, 4695.
71 P. Nabokoff, S. Gastaldi and E. Besson, *Microporous Mesoporous Mater.*, 2021, **311**, 110674.